

# Noise Characterization of Geiger-Mode 4H-SiC Avalanche Photodiodes for Ultraviolet Single-Photon Detection

Yurong Wang, Yang Lv, Yong Wang, Qiongqiong Zhang, Sen Yang, Dong Zhou, Hai Lu, E. Wu, and Guang Wu

**Abstract**—We present here the noise properties of the 4H-SiC avalanche photodiodes (APD) operated in Geiger mode. After-pulse events together with the dark count rate were measured at different temperatures. We found that at a certain bias voltage, the after-pulse probability of the 4H-SiC APD was dependent on the incident photon flux. This interesting observation may be useful to build a photon-number resolving detector for the UV regime. Moreover, the after-pulse and the dark counts noise decreased as the temperature dropped from room temperature to  $-40\text{ }^{\circ}\text{C}$  so that the single-photon detection performance of the 4H-SiC APD could be improved by decreasing the operation temperature.

**Index Terms**—Avalanche photodiodes (APDs), photodetectors, silicon carbide (SiC), ultraviolet (UV) single-photon detection.

## I. INTRODUCTION

IN RECENT years, ultraviolet (UV) single-photon detection has attracted a lot of research interest due to the numerous important applications of the ultra-low-level UV light detection, such as biological-agent detection, deep-space UV astronomy, environmental monitoring, discharge monitoring via UV fluorescent detection [1]. The photomultiplier tubes (PMTs) and microchannel plates (MCPs) are widely used for the single-photon detection and imaging in UV regime [2]–[4]. However, disadvantages including low quantum efficiency of the photocathode for UV light, high voltage, vacuum operation condition, sensitivity to magnetic field and large size, prevent such devices from wide applications. In the last decades, with the development of the materials science, the 4H-SiC avalanche photodiode (APD) is promised to be one of the best UV detector candidates owing to its high quantum efficiency and low dark current [5]–[8]. And the UV single-photon detection has been realized based on 4H-SiC APDs operated in Geiger mode [9]–[14]. As

Manuscript received May 31, 2017; revised August 3, 2017; accepted August 4, 2017. Date of publication August 8, 2017; date of current version August 17, 2017. This work was supported by the National Key Technologies R&D Program of China (2016YFB0400904). (Corresponding author: Guang Wu.)

Y. Wang, Y. Lv, Y. Wang, Q. Zhang, E. Wu, and G. Wu are with the State Key Laboratory of Precision Spectroscopy, East China Normal University, Shanghai 200062, China (e-mail: 986145648@qq.com; 2806504130@qq.com; 1587913240@qq.com; 279914341@qq.com; ewu@phy.ecnu.edu.cn; gwu@phy.ecnu.edu.cn).

S. Yang, D. Zhou, and H. Lu are with the Jiangsu Provincial Key Laboratory of Advanced Photonic and Electronic Materials, and School of Electronic Science and Engineering, Nanjing University, Nanjing 210093, China (e-mail: tzyangsen@163.com; tiandongzhou@126.com; hailu@nju.edu.cn).

Color versions of one or more of the figures in this paper are available online at <http://ieeexplore.ieee.org>.

Digital Object Identifier 10.1109/JSTQE.2017.2737584

the first demonstration of the 4H-SiC APD in the single-photon detection, the detection efficiency was reported to be about 3% at around 300 nm with the dark count rate higher than  $6 \times 10^5$  counts per second (cps) [10]. Since then, efforts have been made to increase the detection efficiency to 10% around 266 nm with the dark count rate of  $2 \times 10^5$  cps [11]–[13]. Recently, Ref. [14] reported the single-photon detection based on 4H-SiC APD at high temperature up to  $150\text{ }^{\circ}\text{C}$ . The detection efficiency dropped slightly around 0.2% while the dark count rate increased from  $20 \times 10^3$  cps to  $80 \times 10^3$  cps, with the temperature changing from  $25\text{ }^{\circ}\text{C}$  to  $150\text{ }^{\circ}\text{C}$ . All the previous studies reported the detector characterization at high temperatures.

In this paper, we characterized the noise properties of the 4H-SiC APD operated in Geiger mode, including the after-pulse and dark count rate at different temperatures from  $-40\text{ }^{\circ}\text{C}$  to  $55\text{ }^{\circ}\text{C}$ . Interesting phenomenon of the after-pulse probability dependent on the incident photon flux was observed, which may be used to build a photon-number resolving detector for the UV regime. And at low temperatures, both the after-pulse and the dark counts noise decreased, providing the possibility to optimize the single-photon detection performance of the 4H-SiC APD by decreasing the operation temperature.

## II. EXPERIMENTS AND RESULTS

The epitaxial structure of the 4H-SiC APD is shown in Fig. 1(a), which consisted of a thin  $0.1\text{-}\mu\text{m}$  p+ cap layer, a  $0.2\text{-}\mu\text{m}$  p layer, a  $0.5\text{-}\mu\text{m}$  p- layer, and a  $2.0\text{-}\mu\text{m}$  n+ layer grown on n-type 4H-SiC substrate. The device was terminated by using a beveled mesa, which was dry-etched down to the bottom n+ layer based on a photoresist reflow technique. The top mesa edge had a diameter of  $\sim 120\text{ }\mu\text{m}$ . More details on fabrication process can be referred to Ref. [15]. The quantum efficiency (QE) of the 4H-SiC APD at 280 nm was  $\sim 30\text{--}35\%$ . The spectral response QE peak of the 4H-SiC APD was observed to be over 50% at  $\sim 270\text{ nm}$ . The 4H-SiC APD was hermetically sealed in a TO-46 package, and welded on the test circuit directly.

The circuit to operate the 4H-SiC APD in Geiger mode for single-photon detection is shown in Fig. 1(b). The breakdown voltage of this 4H-SiC APD was about  $171.0\text{ V}$  at  $25\text{ }^{\circ}\text{C}$ . A high bias voltage above  $171.5\text{ V}$  was applied on the APD. The APD was passively quenched by a  $200\text{-k}\Omega$  resistor. The amplitude of the avalanche pulse was higher than  $50\text{ mV}$ . Then, a fast comparator was used to discriminate the avalanche pulses from

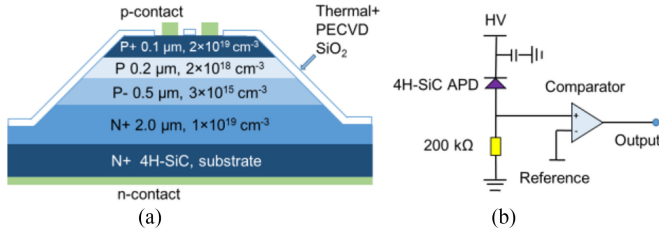


Fig. 1. (a) Device cross section showing beveled edge. (b) Test circuit of the 4H-SiC APD for single-photon detection.

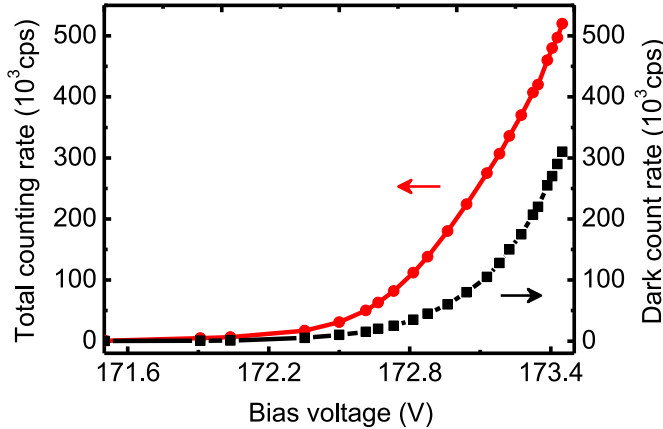


Fig. 2. Total counting rate and the dark count rate as a function of the bias voltage when illuminated by a cw UV light LED.

the background noise. The output of the comparator was a TTL pulse with an amplitude of 5 V. In this way, we could directly get the single-photon counting rate with a counter.

The single-photon detector was characterized with a continuous wave (cw) and a pulsed UV LED, respectively. A bandpass filter at 280 nm with full width at half maximum of 25 nm was used to narrow the emission spectrum of the LED.

Firstly, the cw light source was used to test the single-photon detector based on 4H-SiC APD in free running mode. The UV light was focused onto the APD by a fused silica lens with the focal length of 20 mm. The beam spot at the focus was 60 μm in diameter, which was smaller than the active area of the APD. A calibrated attenuator was placed behind the bandpass filter to attenuate the UV light from 4.16 μW to 2 pW, corresponding to 2.83 × 10<sup>6</sup> photons/s at 280 nm. We increased the bias voltage on the APD step by step and recorded the total counting rate at the output as a function of the bias voltage. The dark count rate of the APD was also recorded without UV light illumination which was dependent on the bias voltage as well. As shown in Fig. 2, when the bias voltage increased from 171.5 V to 173.45 V, the total counting rate increased from 0.5 × 10<sup>3</sup> to 520 × 10<sup>3</sup> cps. But the dark count rate increased rapidly from 0.02 × 10<sup>3</sup> to 310 × 10<sup>3</sup> cps. Note that the total counting rate from the APD did not only contain the useful photon counts but also the after-pulse noise. Usually, the carriers during the avalanching might be captured by the defects in the APDs. And the avalanche pulses might be retriggered when the carriers release, which are called the after-pulse [16]–[17]. When the

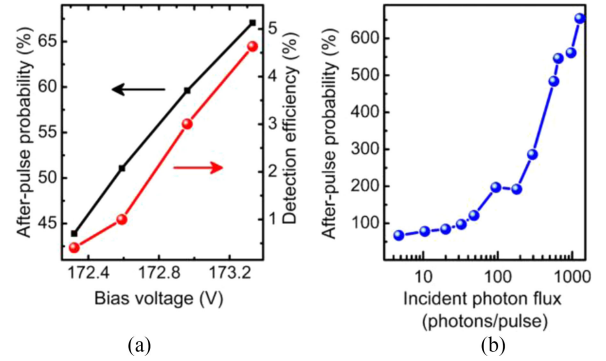


Fig. 3. (a) After-pulse probability and the corrected detection efficiency as a function of the bias voltage when the incident UV pulses contained 5 photons/pulse. (b) After-pulse probability as a function of the incident photon flux when the bias voltage on the 4H-SiC APD was kept at 173.3 V.

after-pulse probability was high, the detection efficiency could not be obtained directly in this free-running mode.

To investigate the after-pulse noise properties of the 4H-SiC APD, we replaced the cw UV LED with a pulsed UV LED. The UV LED was modulated by a signal generator with a repetition rate of 20 kHz. The pulse duration was about 40 ns. The synchronous signal from the signal generator was used as the trigger for the gated photon counter (SR400, Stanford Research Systems, Inc). The gate width of the counting gate was 50 ns, and the dead time of the 4H-SiC APD was at least 300 ns. The possibility of after pulsing happening within the counting gate was very low so that it could be neglected. In this way, the photon detection within the counting gate could be obtained while the counts caused by the after-pulse noise could be analyzed. The UV light pulse was attenuated to contain about 5 photons/pulse and focused on the APD. The after-pulse probability was calculated by

$$P_{\text{after}} = \frac{C_{\text{total}} - C_{\text{gate}} - C_{\text{dark}}}{C_{\text{gate}}}, \quad (1)$$

where  $C_{\text{total}}$  is the total counting rate including the photon counts, dark counts, and after pulses,  $C_{\text{dark}}$  is the dark count rate which is the total counting rate without any input photons, and  $C_{\text{gate}}$  is the count rate within the counting gate of the photon pulses. The black squares in Fig. 3 show the total after-pulse probabilities during the whole period of the photon pulses (~50 μs) when the bias voltage was tuned from 172.3 to 173.3 V. The after-pulse probability increased from 43.9% to 67.1% linearly. Therefore, taking into account the Poisson distribution of the incident photons, the detection efficiency could be corrected as shown by the red round spots in Fig. 3. The detection efficiency increased from 0.4% to 4.6% as the bias voltage increased. The after-pulse and the detection efficiency both increased with the bias voltage of the 4H-SiC APD. The detection efficiency increases with the bias voltage in a certain range in most of the Geiger-mode APDs, because the avalanche probability will increase with the electric field. Usually, the after-pulse probability will decrease, as it will speed up the carriers to release from the defects when the electric field increases in most of the Si APDs and the InGaAs APDs. In these APDs,

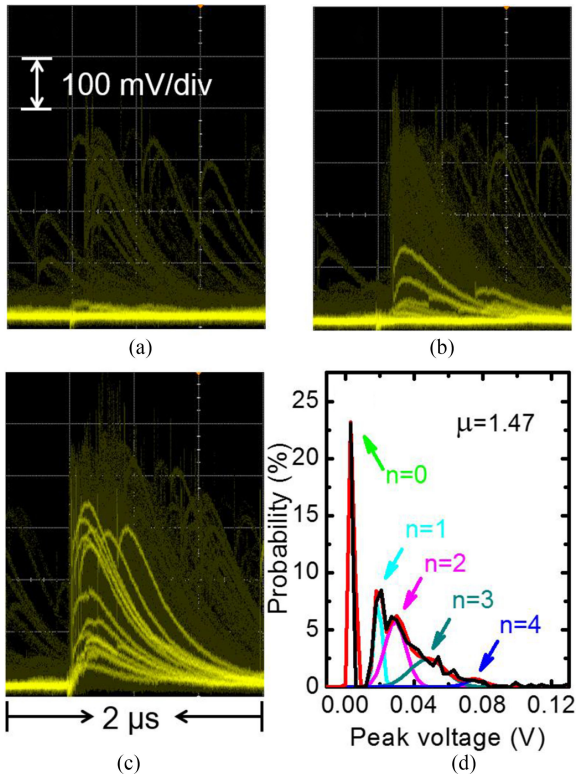


Fig. 4. (a)–(c) Avalanche pulse waveform recorded by the oscilloscope with incident photon flux of 1 photons/pulse, 20 photons/pulse and 100 photons/pulse, respectively. (d) Peak output voltage distribution with detected average photon number of 1.47 photons/pulse.

the avalanche probability increases with the electric field, but the avalanche gain is close to be saturated, so the number of carriers through the APD remains constant, approximately. However, in this experiment, the avalanche gain of the 4H-SiC APD increased with the electric field, so the number of carriers through the APD increased, leading to the increase of the after-pulse probability. Considering the dark count rate, we set the bias voltage at 173.3 V for the rest tests.

We found an interesting phenomenon when measuring the after-pulse probability dependence on the incident photon flux. Usually, the after-pulse probability won't increase with the incident photon flux in Si APDs because the amplitude of the avalanche pulse is a constant. Unlike the Si APD, the after-pulse probability of the 4H-SiC APD increased with the incident photon flux and kept increasing even when the detector was saturated with the incident photon flux beyond 20 photons/pulse as shown in Fig. 3(b).

In order to find out the reason, we used an oscilloscope probe to check the avalanche pulse shape before the signal was sent to the comparator for reshaping. As shown in Fig. 4(a)–(c), the amplitude of the avalanche pulse varied in a large range with the incident photon flux increasing. The maximum avalanche pulse signal could reach 550 mV while the minimum was only 15 mV.

At the first glance, the phenomenon could be explained by the unequal avalanche gain distribution on the 4H-SiC APD active area. If the photons arrived at different positions of the

4H-SiC APD, the avalanche gain change would result in the avalanche pulse shape variation. But if we take close look at those waveforms, we will find that it may not be the whole truth. When the incident photon flux was low, the amplitude of the avalanche pulse was not unique as shown in Fig. 4(a). With the incident photon flux increasing, the amplitude of the avalanche pulse kept increasing even when the incident photon flux reached 100 photons/pulse as shown in Fig. 4(c). No saturation was observed on the avalanche pulse amplitude. If there is just unequal avalanche gain on the 4H-SiC APD, the amplitude of the avalanche pulse should not increase when it is saturated with large incident photon flux which would erase the unequal avalanche gain. Therefore, the pulse amplitude variation was not caused only by the unequal avalanche gain.

Then, the phenomenon should be attributed to the multi-avalanche effect. The avalanche gain may be localized on a small area so that it could be resolved spatially. Multi-avalanche might happen when multi-photon incidents on different areas of the APD [18]. Then the amplitude of the avalanche pulse would be dependent on the incident photon number per pulse. And the after-pulse signal caused by the carrier releasing would also be dependent on the detected photon number per pulse, which explains the increase of the after-pulse probability. As shown in Fig. 4(d), when the average detected photon number was 1.47 photons/pulse, different photon number states of  $n = 1, = 2, = 3$  and  $\geq 4$  could be roughly recognized by the amplitude of the avalanche pulse. The experimental result is displayed as the black line and the simulation according to the Poissonian distribution is shown by the red line [19], indicating that the experimental data fitted exactly the Poissonian superposition of photon-number states. This interesting phenomenon would be helpful to build a photon-number resolving detector in the UV regime.

For further investigation, we placed the 4H-SiC APD together with the pulsed UV light source in a temperature test box. The incident photon flux was kept at about 960 photons/pulse. And the detection efficiency of the APD was kept at 4.6% by tuning the bias voltage. The temporal distribution of the after-pulse events at different temperatures was recorded by a time-correlated single-photon counting (TCSPC) system (HydraHarp 400, PicoQuant GmbH). The resolution of the TCSPC system was set at 32.8 ns. And the acquisition time was about 20 s. The histogram of the after-pulse events is shown in Fig. 5. With the temperature dropped from 55 °C to –40 °C, the after-pulse events decreased but decayed slowly with time at low temperatures. It is well-known that the process of carrier releasing in the defects prolongs at low temperatures, which will also prolong the after-pulse effect. As shown by the black curve in Fig. 5, the after-pulse events decayed very quickly when the temperature of the APD was 55 °C, indicating the fast releasing of the re-triggered carriers. The after-pulse behavior of the 4H-SiC APD at different temperatures is quite similar to that of Si APDs and InGaAs APDs.

The dark count rate of the 4H-SiC APD was measured at different temperatures as well. The bias voltage on the APD was tuned at different temperatures to keep the same total counting rate with the same incident photon flux. The dark count rate

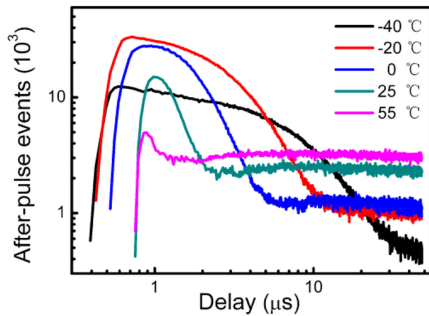


Fig. 5. Histogram of the after-pulse events of the 4H-SiC APD operated at different temperatures measured by a TCSPC system with a resolution of 32.8 ns and an acquisition time of 20 s.

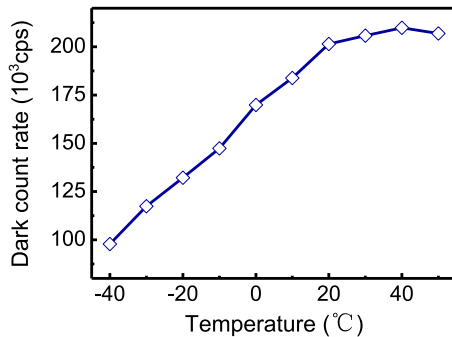


Fig. 6. Dark count rate of the 4H-SiC APD at different temperatures.

as a function of the operation temperature is shown in Fig. 6. The dark count rate was about  $97.7 \times 10^3$  cps at  $-40$  °C, and then increased to  $200 \times 10^3$  cps at  $20$  °C, but varied slightly from  $20$  °C to  $50$  °C. Therefore, although the previous research proved that the main dark counts of 4H-SiC APDs come from the tunneling effect [20]–[22], by decreasing the operation temperature the dark count rate of the 4H-SiC APD could be much reduced.

### III. CONCLUSION

In conclusion, the noise characters of the UV single-photon detector based on 4H-SiC APD operated in Geiger mode were studied in a large temperature tuning range from  $-40$  °C to  $55$  °C. Unlike the Si APD, the after-pulse probability of the 4H-SiC APD increased as the incident photon flux, indicating that the multi-avalanche effect happened during the photodetection. This interesting finding may help to construct a UV photon-number resolving detector based on 4H-SiC APDs. And when the operation temperature was tuned from  $55$  °C to  $-40$  °C, both the after-pulse and the dark counts noise decreased. Therefore, the single-photon detection performance of the 4H-SiC APD could be improved by working at low temperatures.

### REFERENCES

- [1] M. Razeghi and A. Rogalski, "Semiconductor ultraviolet detectors," *J. Appl. Phys.*, vol. 79, no. 10, pp. 7433–7473, May 1996.
- [2] C. D. Granz, B. J. Schindler, G. W. Peterson, and J. E. Whitten, "A fiber optic, ultraviolet light-emitting diode-based, two wavelength fluorometer for monitoring reactive adsorption," *Rev. Sci. Instrum.*, vol. 87, no. 3, Mar. 2016, Art. no. 035121.

- [3] P. Nevodovskyi *et al.*, "Tiny ultraviolet polarimeter for earth stratosphere from space investigation," in *Proc. IEEE 8th Int. Conf. Intell. Data Acquisition Adv. Comput. Syst.: Technol. Appl.*, Berlin, Germany, Sep. 2015, vol. 1, pp. 28–32.
- [4] J. G. Timothy, "Microchannel plates for photon detection and imaging in space," in *Observing Photons in Space*. New York, NY, USA: Springer, 2013, pp. 391–421.
- [5] X. Xin *et al.*, "Demonstration of 4H-SiC UV single photon counting avalanche photodiode," *Electron. Lett.*, vol. 41, no. 4, pp. 212–214, Feb. 2005.
- [6] F. Liu *et al.*, "Discrimination voltage and overdrive bias dependent performance evaluation of passively quenched SiC single-photon-counting avalanche photodiodes," *Chin. Phys. Lett.*, vol. 32, no. 8, pp. 088503-1–088503-4, Mar. 2015.
- [7] X. L. Cai *et al.*, "4H-SiC SACM avalanche photodiode with low breakdown voltage and high UV detection efficiency," *IEEE Photon. J.*, vol. 8, no. 5, pp. 1–7, Oct. 2016.
- [8] F. Liu *et al.*, "Passive quenching electronics for Geiger mode 4H-SiC avalanche photodiodes," *Chin. Phys. Lett.*, vol. 32, no. 12, pp. 128501-1–128501-4, Jul. 2015.
- [9] A. Vert, S. Soloviev, J. Fronheiser, and P. Sandvik, "Solar-blind 4H-SiC single-photon avalanche diode operating in Geiger mode," *IEEE Photon. Technol. Lett.*, vol. 20, no. 18, pp. 1587–1589, Sep. 2008.
- [10] A. L. Beck *et al.*, "Geiger mode operation of ultraviolet 4H-SiC avalanche photodiodes," *IEEE Photon. Technol. Lett.*, vol. 17, no. 7, pp. 1507–1509, Jul. 2005.
- [11] X. G. Bai, D. McIntosh, H. D. Liu, and J. C. Campbell, "Ultraviolet single photon detection with Geiger-mode 4H-SiC avalanche photodiodes," *IEEE Photon. Technol. Lett.*, vol. 19, no. 22, pp. 1822–1824, Nov. 2007.
- [12] X. G. Bai, X. Y. Guo, D. C. McIntosh, H. D. Liu, and J. C. Campbell, "High detection sensitivity of ultraviolet 4H-SiC avalanche photodiodes," *IEEE J. Quantum Electron.*, vol. 43, no. 12, pp. 1159–1162, Dec. 2007.
- [13] X. G. Bai, H. D. Liu, D. C. McIntosh, and J. C. Campbell, "High-detectivity and high-single-photon detection efficiency 4H-SiC avalanche photodiodes," *IEEE J. Quantum Electron.*, vol. 45, no. 3, pp. 300–303, Mar. 2009.
- [14] D. Zhou *et al.*, "High-temperature single photon detection performance of 4H-SiC avalanche photodiodes," *IEEE Photon. Technol. Lett.*, vol. 26, no. 11, pp. 1136–1138, Jun. 2014.
- [15] L. H. Li *et al.*, "High fill-factor 4H-SiC avalanche photodiodes with partial trench isolation," *IEEE Photon. Technol. Lett.*, vol. 28, no. 22, pp. 2526–2528, Nov. 2016.
- [16] A. McCarthy *et al.*, "Kilometer-range depth imaging at 1,550 nm wavelength using an InGaAs/InP single-photon avalanche diode detector," *Opt. Express*, vol. 21, no. 19, pp. 22098–22113, Sep. 2013.
- [17] Y. Liang *et al.*, "Low-timing-jitter single-photon detection using 1-GHz sinusoidally gated InGaAs/InP avalanche photodiode," *IEEE Photon. Technol. Lett.*, vol. 23, no. 13, pp. 887–889, Apr. 2011.
- [18] Z. L. Yuan, J. F. Dynes, A. W. Sharpe, and A. J. Shields, "Evolution of locally excited avalanches in semiconductors," *Appl. Phys. Lett.*, vol. 96, no. 19, Feb. 2010, Art. no. 191107.
- [19] B. E. Kardynal, Z. L. Yuan, and A. J. Shields, "An avalanche-photodiode-based photon-number-resolving detector," *Nature Photon.*, vol. 2, no. 7, pp. 425–428, Jun. 2008.
- [20] Y. M. Kang *et al.*, "Monolithic germanium/silicon avalanche photodiodes with 340 GHz gain-bandwidth product," *Nature Photon.*, vol. 3, no. 1, pp. 59–63, Dec. 2008.
- [21] M. Cheli, P. Michetti, and G. Iannaccone, "Model and performance evaluation of field-effect transistors based on epitaxial graphene on SiC," *IEEE Trans. Electron Devices*, vol. 57, no. 8, pp. 1936–1941, Aug. 2010.
- [22] X. Y. Guo *et al.*, "Study of reverse dark current in 4H-SiC avalanche photodiodes," *IEEE J. Quantum Electron.*, vol. 41, no. 4, pp. 562–567, Apr. 2005.

**Yurong Wang** received the B.S. degree in physics from Taiyuan Normal University, Taiyuan, Shanxi, China, in 2015. She is currently working towards the Ph.D. degree with the State Key Laboratory of Precision Spectroscopy, East China Normal University, Shanghai, China.

Her main research activity concerns single-photon detection and photon-counting laser ranging.

**Yang Lv** received the B.S. degree in physics from Northeast Normal University, Changchun, Jilin, China, in 2016. She is currently with the State Key Laboratory of Precision Spectroscopy, East China Normal University, Shanghai, China.

Her research interests include the development of high-stability single-photon detectors and photon-counting laser ranging.

**Yong Wang** received the B.S. degree in optical information science and technology from Nantong University, Nantong, Jiangsu, China, in 2014. He is currently working toward the M.S. degree in the State Key Laboratory of Precision Spectroscopy, East China Normal University, Shanghai, China.

His main research direction is single-photon detection.

**Qiongqiong Zhang** received the B.S. degree from the Physics Department of Zhejiang Normal University, Jinhua, Zhejiang, China, in 2016 and started the postgraduate studies in State Key Laboratory of Precision Spectroscopy, East China Normal University, Shanghai, China, in 2017.

Her research interest includes single-photon detection.

**Sen Yang** received the B.S. degree from Nanjing University, Nanjing, China, in 2014. He is currently working toward the M.S. degree in the School of Electronic Science and Engineering, Nanjing University.

His current research interests include design, fabrication, and characterization of 4H-SiC-based optoelectronic devices.

**Dong Zhou** received the Ph.D. degree from Nanjing University, Nanjing, China, in 2014. He is currently working with the School of Electronic Science and Engineering, Nanjing University.

His current research interests include fabrication and characterization of III-V and 4H-SiC optoelectronic devices.

**Hai Lu** received the B.S. and M.S. degrees in physics from Nanjing University, Nanjing, China, and the Ph.D. degree in electrical engineering from Cornell University, Ithaca, NY, USA, in 1992, 1996, and 2003, respectively.

He was with GE Global Research Center, Niskayuna, NY, USA, from 2004 to 2006. In 2006, he joined Nanjing University and is a full Professor of microelectronics. He is currently a Principle Investigator with the Nanjing National Laboratory of Microstructures, Nanjing, China. His particular interest has been in the correlation of device performance with material growth and processing parameters. He has published more than 200 articles, book chapters, and conference papers. His current research interests include growth and characterization of III-nitride semiconductors, photonic devices, and high-power devices.

**E. Wu** received the B.S. and Master's degrees from the Physics Department of East China Normal University, Shanghai, China, in 2001 and 2004, respectively. As a cotutored Ph.D. student, she received the joint Ph.D. degree in science from the East China Normal University, Shanghai, China, and Ecole Normale Supérieure de Cachan, Cachan, France, in 2007.

Her research interests include single-photon generation, single-photon manipulation, and single-photon nonlinear interaction. She is a Researcher Professor in the State Key Laboratory of Precision Spectroscopy, East China Normal University, Shanghai, China, since 2013.

**Guang Wu** received the B.S. and Ph.D. degrees from the Physics Department of East China Normal University, Shanghai, China, in 1998 and 2007, respectively.

His research interests include single-photon detection, photon-counting laser ranging and imaging, and quantum key distribution. He is currently with the State Key Laboratory of Precision Spectroscopy, East China Normal University, Shanghai, China, and became a Research Professor in 2013.